PHOTOSYNTHETICA
International Journal for Photosynthesis Research

DOI 10.32615/ps.2022.032 PHOTOSYNTHETICA 60 (3): 465-475, 2022

Photosynthetic mechanism of high yield under an improved wide–narrow row planting pattern in maize

X.L. GE[*,**], Y.B. CHEN[**], Y. WANG[***], B.C. WANG[**], Q. CHAO[**], Y. YU[#], X.J. GONG[#], Y.B. HAO[#], L. LI[#], Y.B. JIANG[#], G.Y. LV[#], C.R. QIAN[#,+], and C.D. JIANG[**,+]

College of Agriculture, Inner Mongolia University for Nationalities, 028042 Tongliao, China[*]
Photosynthesis Research Center, Key Laboratory of Photobiology, Institute of Botany, Chinese Academy of Sciences, 100093 Beijing, China[**]
Key Laboratory of Mollisols Agroecology, Northeast Institute of Geography and Agroecology, Chinese Academy of Sciences, 130102 Changchun, China[***]
Institute of Crop Cultivation and Farming, Heilongjiang Academy of Agricultural Sciences, 150086 Harbin, China[#]

Abstract

Wide–narrow row maize planting patterns are a popular way to enhance maize yield *via* improving canopy PAR. To further optimize canopy PAR, we designed an improved wide–narrow row planting pattern (R2) based on the principle of the shortest projection length and the longest illumination of objects on the ground. Compared to the traditional wide–narrow row planting pattern (R1), maize yield increased by about 10% in R2. R2 maize had higher PAR, leaf area index, chlorophyll content, and photosynthetic rates than maize grown in R1. Moreover, compared to maize leaves in R1, the carbon assimilation enzymatic activities were also significantly higher in R2. The higher carbon assimilation enzymatic activity in R2 could account for the increased photosynthetic rate. Thus, the improved wide–narrow row planting pattern could improve photosynthetic performance by enhancing the PAR of the plant canopy, which further promotes the ear number and yield in northeast China.

Keywords: gas exchange; net photosynthetic rate; photon duration; photosynthetic enzymes; productivity.

Introduction

Maize is a C_4 plant with high photosynthetic efficiency (Hesketh and Musgrave 1962). The photosynthetically active radiation (PAR) energy-utilization efficiency of maize is only about 1 to 2% at present, which is much lower than the theoretical maximum value of 5 to 6% (Loomis and Williams 1963). Under optimal temperature conditions, maize production in northeast China can theoretically reach 32,000–35,000 kg ha^{-1}, but the current average maize production in the region ranges from 6,750–8,000 kg ha^{-1}, which is about 1/5 of the theoretical output

Highlights

- The improved wide–narrow row planting pattern optimized the canopy light environment
- Optimizing PAR enhanced carbon assimilation enzymatic activity and photosynthetic rate
- The study provided a reference for maize yield improvement in northeast China

Received 12 November 2021
Accepted 30 June 2022
Published online 6 September 2022

[+]Corresponding authors
e-mail: qcr3906@163.com (C.R. Qian)
jcdao@ibcas.ac.cn (C.D. Jiang)

Abbreviations: C_i – intercellular CO_2 concentration; E – transpiration rate; g_s – stomatal conductance; L_I – light interception of the stand; LMA – leaf mass per unit area; LUE – light-use efficiency; MDH – malate dehydrogenase; ME – malic enzyme; N area – nitrogen content per unit area; PEPC – phospho*enol*pyruvate carboxylase; P_N – net photosynthetic rate; PNUE – photosynthetic nitrogen-use efficiency; PPDK – pyruvate orthophosphate dikinase.

Acknowledgments: This study was supported by the National Natural Science Foundation of China, Grant No. 32060435, the United Guiding Project of the Heilongjiang Natural Science Fund, Grant No. LH2019C060, and the State Key Research and Development Plan of China, Grant No. 2017YFD0300505-1.

Conflict of interest: The authors declare that they have no conflict of interest.

based on the PAR–temperature conditions (Gao *et al.* 2011). Thus, the potential maize productivity in northeast China is far from being fully exploited.

The improvement of maize stand photosynthesis production is known to be important for yield improvement. However, a traditional planting pattern with a distance of 0.65 m between ridges and irregular ridge directions has long been used in northeast China. Maize grown in this traditional pattern has low photosynthetic efficiency due to poor PAR and uneven PAR distribution within the stand (Maddonni *et al.* 2001, Zhu *et al.* 2010). Compared to the traditional planting pattern with uniformly-spaced ridges, nonuniform spacing or appropriate spacing ratios can effectively adjust the contradictions between individual plant requirements and the requirements of the entire maize stand. However, the photosynthetic mechanism responsible for the high yield of the wide–narrow maize planting pattern should be clarified (Wu *et al.* 2005, Liang *et al.* 2009, Wang *et al.* 2009, Fan *et al.* 2010, Wei *et al.* 2014, Zhang *et al.* 2015, Zheng *et al.* 2017). In addition, manipulating crop canopy architecture results in the lack of total canopy PAR interception due to incomplete coverage, at least in the early season, which could be a cause of yield reduction in maize (Stewart *et al.* 2003, Hammer *et al.* 2009, Yang *et al.* 2010, Reynolds *et al.* 2011).

In the present study, according to the climate characteristics of northeast China, a planting pattern (R2, with combined ridges spaced 1.60 m apart for wide rows and 0.40 m apart for narrow rows) was designed based on the principle of the shortest projection length and the longest illumination of objects on the ground. It was hypothesized that this pattern could minimize the projection length of an object on the ground and maximize the period of illumination of an object to make the best use of PAR, thus improving photosynthesis and increasing maize yield. Three-year trials were conducted to investigate the effects of the planting pattern on the PAR distribution within the canopy, the photosynthetic parameters, and the carbon assimilation, and explore the photosynthetic mechanism of high yield in the wide–narrow maize planting pattern.

Materials and methods

Natural characteristics of the experimental zone: The experimental area has a temperate continental climate, with an annual average temperature of 4.4°C, annual average rainfall of 520 mm, and a frost-free period of 138 d. The experimental zone contains a thin layer of black soil. The basic physical and chemical properties of this soil are 26.9 g(organic matter) kg^{-1}, 1.20 g(total nitrogen) kg^{-1}, 1.06 g(total phosphorus) kg^{-1}, 16.9 g(total potassium) kg^{-1}, 118 mg(available nitrogen) kg^{-1}, 18.0 mg(available phosphorus) kg^{-1}, 111 mg(available potassium) kg^{-1}, 1.23 g cm^{-3} soil bulk density, and pH 6.6. The mean temperature and precipitation for 2013–2015 are shown in the text table.

The improved wide–narrow row planting pattern and the experimental design: The traditional planting pattern cannot make available most of the PAR and its duration due to the actual terrain, resulting in the problems of insufficient space for crop growth, mutual shading, a short photon duration, and poor PAR quality within the stand. Because of this, we focused on the shortest projection length of objects on the ground and the longest illumination periods in this research (Fig. 1S, *supplement*). The 'ac' in the program stands for crop plant height, which is set to 'L'; the 'ab' in the program stands for crop shadow length, which is set to 'YL'; and the 'db' in the program stands for the width of crop projection, which is set to 'TL':

$$YL = L \times \operatorname{ctg} h$$

$$TL = YL \times \sin(\Phi \pm A) = L \times \operatorname{ctg} h \times \sin(\Phi \pm A)$$

In the formulas above, the 'h' stands for the solar altitude, the 'Φ' stands for the solar azimuth, and the 'A' stands for the angle of the plant and magnetic south direction. As calculated by the formula, when the angle of the plant and the magnetic south direction were 20°, the horizontal projection of the planting line in the testing site was the shortest and the photon flux duration was the longest, and the proportion of the horizontal projection length between 0.00 m and 1.60 m was the largest from 9:30 to 14:30 h. Therefore, the ridge direction of the planting pattern designed in this study is prone to south 20° to west, and the ridge distances were 1.60 m for wide rows and 0.40 m for narrow rows.

Field design: The current study was carried out from May to October from 2013 to 2015 (growing season) at the Experimental Station (44°12'21"N, 125°33'28"E), Northeast Institute of Geography and Agroecology, Chinese Academy of Science in Dehui County, Jilin province, China. Two ridge configurations, consisting of a traditional cultivation planting pattern (R1, a single line with a row spacing of 0.65 m, south to north ridge direction, and 75,000 plants ha^{-1}) and an improved wide–narrow row planting pattern (R2, the narrow rows were 0.40 m wide, the wide rows were 1.60 m wide, the ridge direction was south prone 20° to west, and 75,000 plants ha^{-1}), were tested (Fig. 2S, *supplement*). The experimental maize cultivar used was Liang Yu 99, the sowing period was early May, and the harvest period was at the end of September. Two healthy seeds were planted in each hole, and the fertilizer concentrations were 300 kg(N) ha^{-1}, 90 kg(P) ha^{-1}, and 100 kg(K) ha^{-1}. Testing was performed and compared between large plots, and the single plot area was approximately 0.0667 ha with three replicates. The crops were free from pests, weeds, disease, and irrigation. The other field management practices were the same as those used in normal field production.

Leaf area index: The leaf area of plants in R1 and R2 were determined by selecting three representative observation points in each treatment and five representative plants at the flowering stage at each observation point. The leaf area of all leaves of each plant was calculated using the following formulas (Hou *et al.* 2021):

Leaf area of fully expanded leaf = length × width × 0.75

Leaf area of incompletely expanded leaf = length × width × × 0.50

Month	2013		2014		2015	
	Mean temperature [°C]	Precipitation [mm]	Mean temperature [°C]	Precipitation [mm]	Mean temperature [°C]	Precipitation [mm]
April	11.00	3.90	10.33	11.00	9.02	1.26
May	16.39	52.70	16.85	73.20	17.52	102.26
June	21.01	24.20	22.15	54.70	20.52	116.47
July	24.68	180.60	25.46	65.00	24.40	160.69
August	21.70	234.90	21.75	244.80	21.59	279.43
September	15.85	29.60	15.56	67.90	17.64	31.70
October	7.30	0.20	7.74	38.50	8.75	21.80
Mean/total	16.85	526.10	17.12	555.10	17.06	713.64

The leaf area of each plant was the sum of the leaf area of all fully expanded leaves and the incompletely expanded leaves, and the leaf area index values were calculated using the following formula:

Leaf area index = average leaf area per plant × planting density/10,000

Chlorophyll (Chl): The Chl content of the ears and the other fully expanded leaves of the upper, middle, and lower layers of the plants in R1 and R2 were determined at the grain-filling stage, with three replicates. Leaf discs were collected from both sides of the leaf vein using a punch with a diameter of 1 cm, and a 0.5-g sample was weighed, placed into 80% acetone solution, and extracted in the dark for 24 h (Li *et al.* 2000). The extinction value of the extract was measured at the wavelengths of 663 and 645 nm with a spectrophotometer (*UV-6100*, *MAPADA*, Shanghai, China). The contents of Chl *a* and Chl *b* were calculated using the following formulas:

$$\text{Chl } a \text{ [mg kg}^{-1}\text{(DM)]} = (12.70 \times A_{663} - 2.697 \times A_{645}) \times \times V/(1{,}000W)$$

$$\text{Chl } b \text{ [mg kg}^{-1}\text{(DM)]} = (22.77 \times A_{645} - 4.687 \times A_{663}) \times \times V/(1{,}000W).$$

In the formulas above, A_{663} and A_{645} were the extinction values at corresponding wavelengths, and the V and W were the liquid volumes of extraction value and the mass of the sample, respectively. The content of Chl was the sum of the content of Chl *a* and the content of Chl *b*.

Net photosynthetic rate: The measurement was performed in triplicate on a sunny day using plants at the grain-filling stage. The net photosynthetic rate (P_N) of the ear during one day was determined in R1 and R2 at time points of 8:00, 10:00, 12:00, 14:00, and 16:00 h; the P_N of leaves from 0.50 m, 1.00 m, and 1.50 m canopy layers in R1 and R2 were also determined during the period of 9:00 to 11:00 h by using an *LI-6400 XT* portable photosynthetic apparatus (*LI-COR*, Nebraska, USA) set at a saturated PAR intensity of 1,500 μmol(photon) m^{-2} s^{-1}.

Photosynthetic capacity: The P_N, stomatal conductance (g_s), intercellular CO_2 concentration (C_i), transpiration rate (E), and other ear leaf indicators were determined using an *LI-6400 XT* portable photosynthetic apparatus (*LI-COR*, Nebraska, USA) under a 500 μmol mol^{-1} CO_2 flow rate, a 25°C leaf chamber temperature, and simulated PAR intensities of 1,800; 1,500; 1,200; 1,000; 800, 600, 400, 200, 100, and 0 μmol(photon) m^{-2} s^{-1} from 9:00 to 11:00 h on a sunny day at the grain-filling stage with three replicates.

Effective PAR: The effective PAR of the R1 and R2 treatments was monitored by an environmental radiation temperature and humidity recorder (*Minikin RTHi*, Czech Republic) from 6:00 to 16:00 h at the ear position from two locations in the east and west of one row in the R1 and R2 plots every 40 min on a sunny day during the grain-filling stage.

Photosynthetic enzymes: The activities of ribulose-1,5-bisphosphate carboxylase/oxygenase (Rubisco, EC 4.1.1.39), pyruvate orthophosphate dikinase (PPDK, EC 2.7.9.1), malic enzyme (ME, EC 1.1.1.40), malate dehydrogenase (MDH, EC 1.1.1.37), and phospho-*enol*pyruvate carboxylase (PEPC, EC 4.1.1.31) of the ear leaves from R1 and R2 were determined from samples collected at 6:00, 9:00, 13:00, 16:00, and 20:00 h on a sunny day during the grain-filling stage. The protein concentration was determined using *QuickStartTM Bradford 1XDYE Reagent* (*Bio-Rad*, CA, USA) based on dye binding with crystalline bovine serum albumin as a standard. The specific methods for enzyme activity assays are detailed below.

Rubisco: The Rubisco enzyme assay was performed as previously described with some modifications (Sawada *et al.* 2003, Jin *et al.* 2006). Leaves from different positions were ground to a powder using a chilled mortar and pestle with liquid N_2. Soluble protein extracts for enzyme assays were prepared by homogenizing 0.2-g powdered maize leaves in 400 μL of ice-cold extraction buffer containing 50 mM Tris–HCl (pH 7.5), 1 mM EDTA, 10 mM $MgCl_2$, 12% (v/v) glycerol, 0.1% (v/v) 2-mercaptoethanol, 1% (w/v) PVP-40, and 1% *Sigma* protease cocktail. The homogenate was clarified by 20-min centrifugation at 20,000 × *g* and 4°C. The concentration and activity of Rubisco were determined by adding 5 μL of supernatant to 900 μL of assay buffer containing 50 mM HEPES–

KOH (pH 8.0), 1 mM EDTA, 20 mM $MgCl_2$, 2.5 mM dithiothreitol (DTT), 10 mM $NaHCO_3$, 5 mM ATP, 0.2 mM NADH, 5 mM creatine phosphate, 0.5 mM RuBP, 10 U of phosphocreatine kinase, 10 U of glyceraldehyde-3-phosphate dehydrogenase, and 10 U of phosphoglycerate kinase, followed by incubation at 30°C for 20 min. NADH oxidation was monitored at 340 nm in a dual-beam UV spectrophotometer (*UV-2550*, *Shimadzu*, Kyoto, Japan). Rubisco activity was expressed as the amount of enzyme that catalyzed 1 micromole of substrate per minute per miligram fresh mass.

PPDK: Soluble protein extracts for enzyme assays were prepared by homogenizing 0.5 g of maize leaves in 500 µL of ice-cold extraction buffer containing 50 mM HEPES (pH 8.0), 10 mM $MgCl_2$, 0.1 mM EDTA, 5 mM Glc 6-PNa_2, 10 mM $NaHCO_3$, 10 mM dithiothreitol, 2.5 mM KH_2PO_4, and 5 mM $(NH_4)_2SO_4$. The homogenate was clarified by centrifugation for 20 min at 20,000 × *g* and 4°C. Aliquots of the extracts were assayed for PPDK activity using a coupled PEPC/malate dehydrogenase-based spectrophotometric assay. To each aliquot, 2 mM pyruvate, 1.25 mM ATP, 0.2 mM NADH, 12 U malate dehydrogenase, and 0.5 U phospho*enol*pyruvate carboxylase were added (Chastain *et al.* 2000). After incubation at 30°C for 20 min, NADH oxidation was monitored at 340 nm in a dual-beam UV spectrophotometer (*UV-2550*, *Shimadzu*, Kyoto, Japan). PPDK activity was expressed as the amount of enzyme that catalyzed 1 micromole of substrate per minute per miligram fresh mass.

ME: The standard reaction mixture contained 100 mM Tris–HCl pH 8.0, 10 mM $MgCl_2$, 0.5 mM NADP, and 4 mM L-malate. The reaction was started by the addition of L-malate. ME activity was measured spectrophotometrically at 30°C by monitoring NADPH production at 340 nm. One unit was defined as the amount of enzyme that catalyzed the formation of 1 mmol of NADPH min^{-1}.

The kinetic parameters of ME were also obtained after treatment with either 10 mM DTT (redZmC_4-NADP-ME) for 2 h or 2 mM diamide (oxZmC_4-NADP-ME) for 20 min at 0°C. After both treatments, the enzyme was desalted using *Microcon-30* (*Millipore*, *42404*, MA, USA) columns with 100 mM Tris–HCl pH 8.0 and 10 mM $MgCl_2$ (Alvarez *et al.* 2012). After incubation at 30°C for 20 min, NADH oxidation was monitored at 340 nm in a dual-beam UV spectrophotometer (*UV-2550*, *Shimadzu*, Kyoto, Japan). ME activity was expressed as the amount of enzyme that catalyzed 1 micromole of substrate per minute per miligram fresh mass.

MDH: The extraction procedure was carried out at room temperature using a chilled mortar with tissue grinding medium, containing 0.1 M Tris–HCl (pH 7.5 and 4°C), 10 mM $MgCl_2$, 1 mM EDTA, and 5% (w/w of leaf tissue) polyvinylpolypyrrolidone. The tissue was ground for 1.5 to 2 min and the homogenate was filtered through *Miracloth* (*Millipore*, MA, USA). To assay MDH activity, a 25-µL aliquot of the homogenate was added to the reaction mixture (25 mM Tris–HCl, pH 8.0, 1 mM EDTA, and 0.2 mM NADPH) and centrifuged at 14,000 × *g*. The supernatant was assayed immediately at 25°C as previously described. The reaction was initiated by the addition of oxalacetate (0.5 mM) and the oxalacetate-dependent (Nakamoto and Edwards 1983). After incubation at 30°C for 20 min, NADH oxidation was monitored at 340 nm in a dual-beam UV spectrophotometer (*UV-2550*, *Shimadzu*, Kyoto, Japan). MDH activity was expressed as the amount of enzyme that catalyzed 1 micromole of substrate per minute per miligram fresh mass.

PEPC: PEPC activity was measured spectrophotometrically as described by Takahashi-Terada *et al.* (2005) with some modifications. Leaves from different positions were ground to a powder using a chilled mortar and pestle with liquid N_2. Soluble protein extracts for enzyme assays were prepared by homogenizing 0.2-g powdered maize leaves in 400 µL of ice-cold extraction buffer containing 100 mM Tris–HCl (pH 7.5), 1 mM EDTA, 10 mM $MgCl_2$, 20% (v/v) glycerol, 14 mM 2-mercaptoethanol, and 1% *Sigma* protease cocktail. The homogenate was clarified by centrifugation for 20 min at 20,000 × *g* and 4°C. The supernatant was used to determine the concentration and activity of PEPC in a 1.0-mL reaction mixture containing 50 mM HEPES–NaOH (pH 8.0), 5 mM $KHCO_3$, 10 mM $MgCl_2$, 0.25 mM EDTA, 2 mM DTT, 0.1 mM NADH, and 10 U ml^{-1} of MDH. The reaction was initiated by the addition of 2 mM PEP at 30°C. NADH oxidation was monitored at 340 nm in a dual-beam UV spectrophotometer (*UV-2550*, *Shimadzu*, Kyoto, Japan). PEPC activity was expressed as the amount of enzyme that catalyzed 1 micromole of substrate per minute per miligram fresh mass.

Photosynthetic nitrogen-use efficiency: The P_N values of ear leaves and the seven leaves above and below the ear in R1 and R2 were determined using an *LI-6400 XT* portable photosynthetic apparatus (*LI-COR*, Nebraska, USA) from 8:30 to 11:30 h on a sunny day at the grain-filling stage with three replicates. All the leaves were clipped after the determination of P_N, and the leaf area of each leaf was determined by using an *LI-3000C* portable leaf area apparatus (*LI-COR*, Nebraska, USA). Then, all the leaf samples were dried to constant mass, and the nitrogen content of each leaf (N_{leaf}) was determined using the method described by Yan *et al*. (2011) with three replicates. The following formulas were used (Zhu *et al.* 2018):

Leaf mass per unit area (LMA [g m^{-2}]) = leaf dry mass/leaf area

Nitrogen content per unit area (N_{area} [g m^{-2}]) = N_{leaf} × × LMA/100

Photosynthetic nitrogen-use efficiency (PNUE [µmol g^{-1} s^{-1}] = P_N/N_{area}

The final formula was constructed according to the formula in the section 'Leaf area index'.

Aboveground biomass: The aboveground biomass was measured every 10 d after maize flowering by selecting three representative observation points in each treatment. Five representative plants with uniform growth were selected at each observation point. The samples were collected and placed in a ventilated drying oven at 105°C for 30 min, then dried to a constant mass at 80°C, and the dry mass of a single plant was measured.

Light energy-use efficiency: The PAR values of the top (I_0) (30 cm above the canopy) and bottom (I) of the canopy of R1 and R2 were measured using a linear light quantum meter (*LI-COR*, Nebraska, USA) every 2 h from 6:00 to 18:00 h on a sunny day at the grain-filling stage with three replicates. The mean value of seven results in a day represented the light interception rate of the stand in this growth period. In addition, it was assumed that half of the total solar radiation was photosynthetic effective radiation (PAR) (Zhao *et al.* 2018, Hu *et al.* 2020). The following formulas were used to calculate:

Light interception of the stand ($[L_I$ [%]) = $(I_0 - I)/I \times 100$ (Tang *et al.* 2012)

Light energy-use efficiency (LUE [g MJ^{-1}]) = DMW/PAR × × $L_I \times N_d$ (Tsubo *et al.* 2001)

In the formula above, DMW refers to the dry matter accumulation above ground after anthesis to the grain-filling stage (40 d after anthesis) of maize plants, and N_d is the number of days of the corresponding growth period (40 d from anthesis to the grain-filling stage).

Yield: Ears in every single plot of R1 and R2 were all harvested and threshed, and the grain mass was measured with three replicates.

Statistical analysis: All statistical data were analyzed using *Excel* and *SPSS 22.0*. Graphs were constructed using *Origin 2022* software. The two-independent-samples tests (nonparametric tests) were used to analyze the significant differences between the measured data by *Mann-Whitney*'s *U*. The significance level was the $p<0.05$ level.

Results

Comparison of the yield and yield components: Analysis of two-independent-samples tests showed that the planting pattern had significant effects on the ear number and yield. The average yield of maize grown in R1 in each year from 2013 to 2015 was always lower than that of R2, and the differences between the yields of R1 and R2 were significant in 2013 and 2014. Compared with R1, the yields of R2 were 18.4, 18.6, and 15.3% higher in 2013, 2014, and 2015, respectively. The ear number was also higher in R2, and increased by 14.4, 14.6, and 11.4% compared with R1 in 2013, 2014, and 2015, respectively; the differences between the ear number of R1 and R2 were also significant in 2013 and 2014, while there was little difference in kernels per ear and 1000-kernel mass, indicating that the ear number was the key factor in the yield improvement of R2 (Table 1).

Characteristics of the leaf sources of different planting patterns: The leaf area index of maize grown in R2 was higher and increased by 10.0% compared with that of R1, and the difference was significant (Fig. 1*A*). The content of Chl was also higher in R2 and increased by 5.7% compared with that of R1, and the difference was also significant (Fig. 1*C*). However, there was little difference in the leaf mass per unit area and the photosynthetic nitrogen-use efficiency of maize between the two planting patterns (Fig. 1*B*,*D*).

Gas-exchange characteristics: When PAR was in the range of 0–200 μmol(photon) m^{-2} s^{-1}, the P_N of plants grown in both R1 and R2 increased with increasing photon flux density, but the differences were not significant; when the PAR was in the range of 200–1,500 μmol(photon) m^{-2} s^{-1}, the P_N of R2 was higher than that of R1; and when the PAR was greater than 1,500 μmol(photon) m^{-2} s^{-1}, the P_N of R1 reached saturation and then fell slightly, while the P_N of R2 remained high (Fig. 2*A*). The characteristics of stomatal conductance and transpiration rate under different planting patterns both exhibited similar trends to that of the net photosynthetic rate (Fig. 2*B*,*D*). As the PAR increased from 0–1,800 μmol(photon) m^{-2} s^{-1}, the intercellular CO_2 concentration of plants in each planting pattern gradually declined. When the PAR was greater than 1,200 μmol(photon) m^{-2} s^{-1}, the intercellular CO_2 concentration of R2 plants was still higher than that of R1 plants (Fig. 2*C*). The P_N of the ear leaf, which was measured during the grain-filling stage, was higher for plants grown in R2 than that in R1, increasing rapidly in the morning and decreasing slowly in the afternoon. Due to the better PAR conditions, the P_N of the ear leaf of R2

Table 1. Yield and yield components of different planting patterns from 2013 to 2015. Data are means ± SE ($n = 3$). *Different lowercase letters* indicate statistically significant differences at the $p<0.05$ level.

Year	Treatment	Ear number [ha^{-1}]	Kernels per ear	1000-kernel mass [g]	Yield [kg ha^{-1}]
2013	R1	59,467 ± 930^b	499 ± 8^a	301.7 ± 4.7^a	10,020 ± 157^b
	R2	68,010 ± 2,066^a	518 ± 16^a	305.0 ± 9.3^a	11,862 ± 360^a
2014	R1	60,581 ± 1,121^b	508 ± 9^b	307.3 ± 5.7^a	10,208 ± 189^b
	R2	69,428 ± 1,270^a	529 ± 10^a	311.4 ± 5.7^a	12,110 ± 222^a
2015	R1	59,952 ± 844^b	503 ± 7^a	304.1 ± 4.3^a	10,102 ± 142^b
	R2	66,791 ± 6,207^a	509 ± 47^a	299.5 ± 27.8^a	11,650 ± 1,083^a

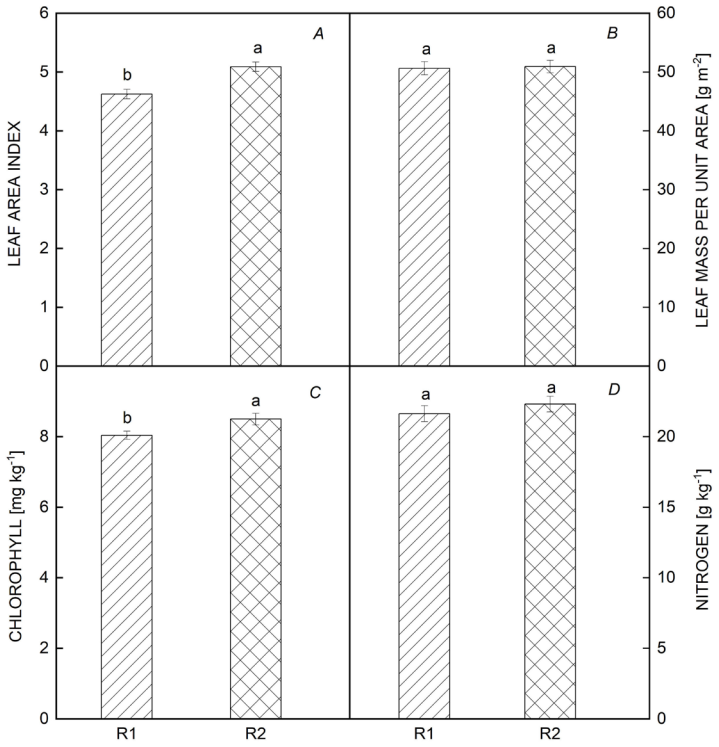

Fig. 1. Comparisons of leaf area index (*A*), leaf mass per unit area (*B*), chlorophyll content (*C*), and nitrogen content (*D*) at different planting patterns. Data are means ± SE ($n = 3$), *different lowercase letters* indicate statistically significant differences at the $p<0.05$ level.

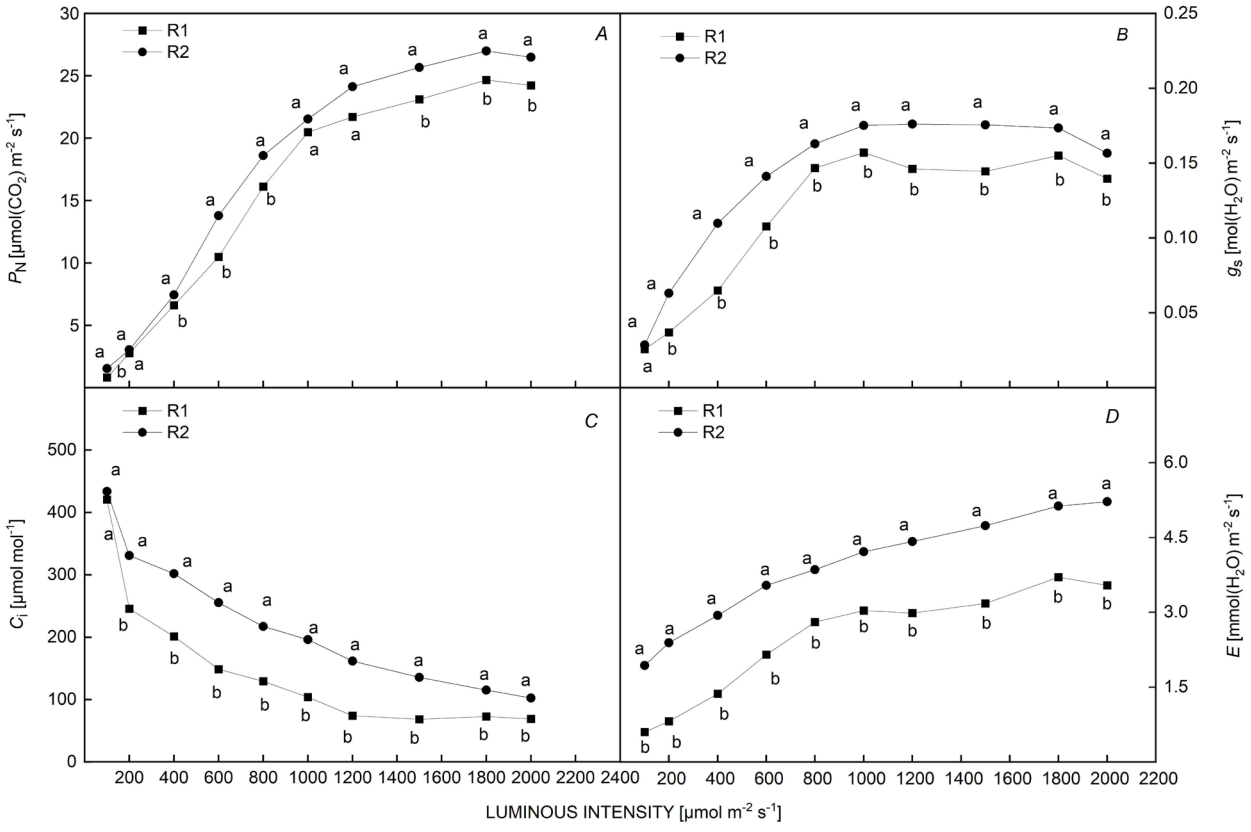

Fig. 2. Changes in the net photosynthetic rate (P_N) (*A*), stomatal conductance (g_s) (*B*), intercellular CO_2 concentration (C_i) (*C*), and transpiration rate (*E*) (*D*) of different planting patterns. Data are means ± SE ($n = 3$), *different lowercase letters* indicate statistically significant differences at the $p<0.05$ level.

plants was 2.26 μmol(CO_2) m^{-2} s^{-1} higher than that of R1 plants at 12:00 h, and 6.8 μmol(CO_2) m^{-2} s^{-1} higher at 16:00 h (Fig. 3*A*). The P_N values of leaves located at a different position on the plant were further measured. Compared with R1, the P_N of R2 leaves was 17.2, 13.2, and 12.6% higher for leaves located at 150 cm, 100 cm, and 50 cm from the base of the plant, respectively, and the differences were all highly significant (Fig. 3*B*).

PAR intensity characteristics: The PAR received by maize leaves of R1 was always lower than that of R2 from 6:00 to 16:00 h each day. Maize grown in R2 received more solar energy than R1 from 8:30 to 12:00 h and from 13:30 to 15:30 h, and the mean PAR received by maize leaves of R2 was 4.93 times and 2.89 times that of R1 during these two time periods, respectively, which indicated that R2 plants received more PAR energy for photosynthesis (Fig. 4).

The activity of key photosynthetic enzymes: The activity of Rubisco was higher in R2. The highest activities of Rubisco and PPDK were observed between 9:00 and 16:00 h, and the highest enzymatic activity in R2 plants was approximately twice that of R1 plants (Fig. 5*A*,*B*). MDH catalyzes the reversible conversion between malic acid and oxaloacetic acid, which was the highest in R2 plants from 9:00 to 16:00 h (Fig. 5*C*). The activity of ME, which catalyzes malic acid oxidative decarboxylation to produce pyruvic acid and CO_2, was the highest in R2 from 9:00 to 16:00 h (Fig. 5*D*). The activity of PEPC, which is the main rate-limiting enzyme of the C_4 cycle, was nearly two times higher in R2 plants than that in R1 plants, and the highest activity was maintained for about 7 h (Fig. 5*E*). In general, the activities of Rubisco, PPDK, ME, MDH, and PEPC of R2 in the whole day increased by 65.0, 67.2, 33.9, 18.6, and 25.2%, respectively, compared with R1.

Due to the change in ridge distance, plants grown in the R2 pattern developed higher light energy-use efficiency and photosynthetic performance (Fig. 6), which could promote the activity of photosynthetic carbon motabolism. enzymes.

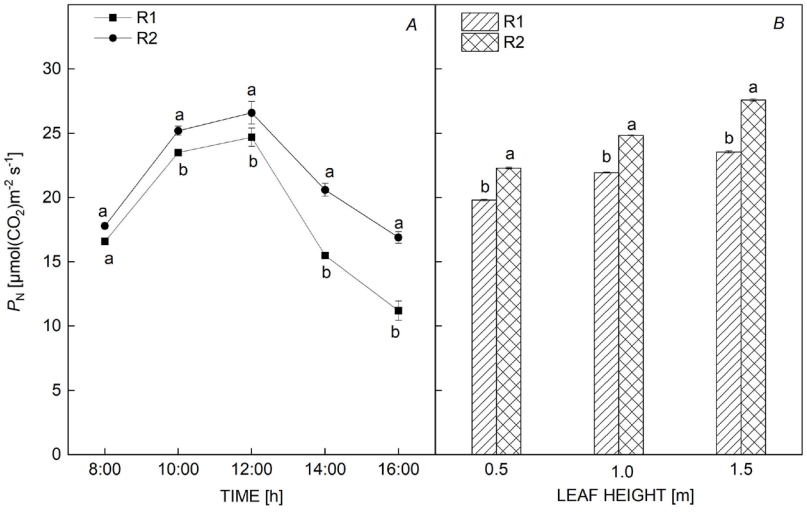

Fig. 3. The net photosynthetic rate (P_N) of maize ear leaves (*A*) and leaves (*B*) at different heights at different planting patterns. Data are means ± SE (n = 3), *different lowercase letters* indicate statistically significant differences at the $p<0.05$ level.

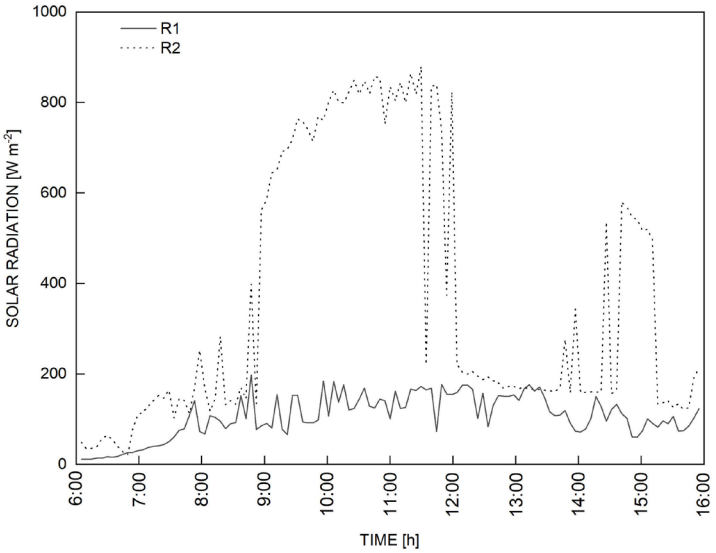

Fig. 4. The mean PAR irradiance received by maize leaves of different planting patterns.

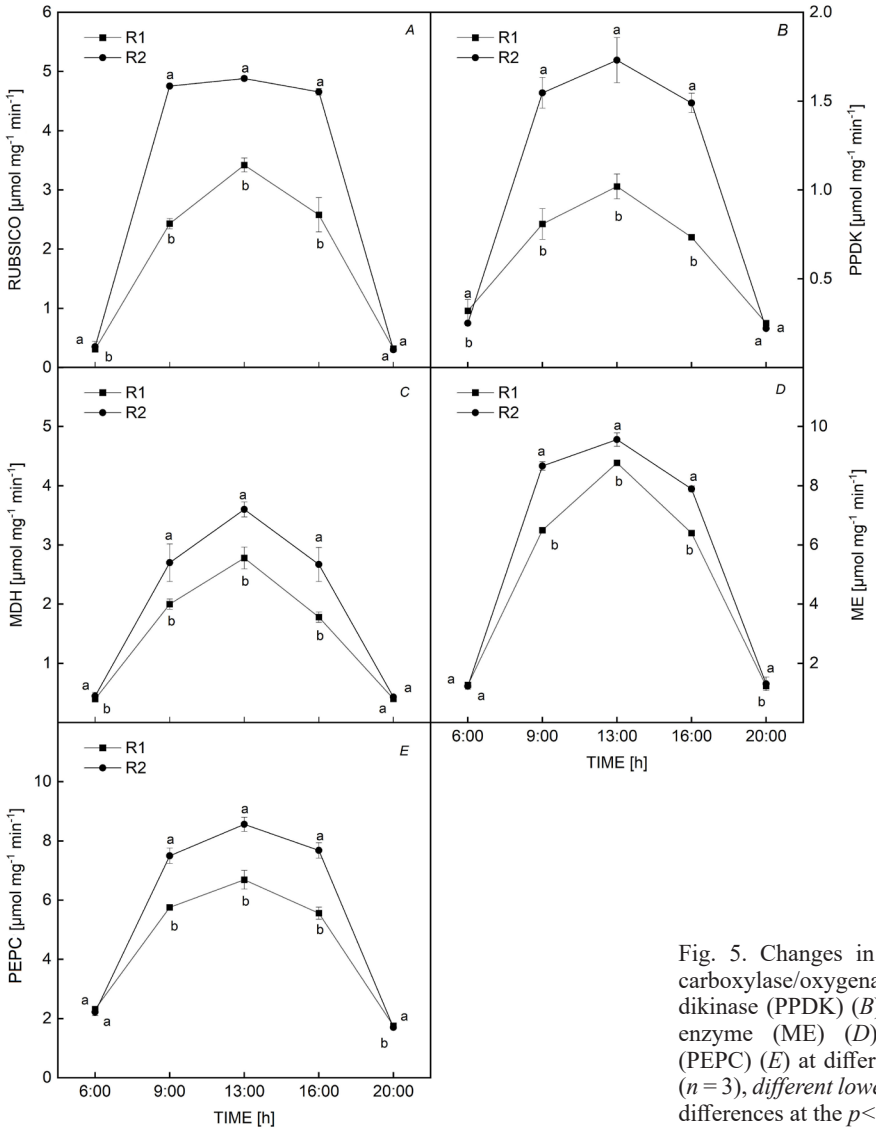

Fig. 5. Changes in the activities of ribulose-1,5-bishosphate carboxylase/oxygenase (Rubisco) (*A*), pyruvate orthophosphate dikinase (PPDK) (*B*), malate dehydrogenase (MDH) (*C*), malic enzyme (ME) (*D*), and phospho*enol*pyruvate carboxylase (PEPC) (*E*) at different planting patterns. Data are means ± SE ($n = 3$), *different lowercase letters* indicate statistically significant differences at the $p<0.05$ level.

Discussion

Row distance is important for crop canopy structure (Yang *et al.* 2010, Xiao *et al.* 2017, Xu *et al.* 2017). Improved canopy structure can lead to better interception of solar radiation, and consequently, increase PAR availability. The use of uniform ridges results in low PAR at the middle and base of the plants in traditional maize planting patterns. Compared to the traditional planting pattern, the wide and narrow row planting pattern promotes the leaf area index, Chl content, and PAR interception capacity of the ear-leaf layer. The P_N of the whole crop stand increases, as does the grain yield (Yang *et al.* 2010, Liu *et al.* 2014, Bai *et al.* 2019, 2020; Zhang *et al.* 2020, Li *et al.* 2021). In this study, it was found that maize leaves located at the middle and base of plants grown in R2 received more PAR and extended illumination time (Fig. 4) than plants grown in R1, which allowed these plants to receive more PAR for photosynthesis.

The photosynthetic performance of the blade is another important indicator of maize yield formation (Yu *et al.* 1998, Zhang *et al.* 2012, Jia *et al.* 2020, Jin *et al.* 2020). The production of photosynthetic material mainly depends on photosynthetic efficiency and the duration of green leaves after flowering (Dai *et al.* 2008, Lin *et al.* 2008, Li *et al.* 2009). In this study, it was found that the P_N values of plants in the R2 pattern were higher than that in R1, which was more obvious at the bottom of the stand canopy (Fig. 3). PAR-response curves reflect the changes in photosynthetic rate with changing PAR intensity and are useful for determining plant photosynthetic capacity (Shimazaki *et al.* 2007, Liu *et al.* 2018). Due to the change in ridge distance, plants grown in the R2 pattern received more sun PAR for longer periods than R1, which allowed plants to develop higher light energy-use efficiency (Fig. 6*A*). It was also found that the nitrogen content of maize leaves for plants grown in R2 increased slightly compared to R1 based on the improvement of photosynthesis performance (Fig. 1), while the photo-

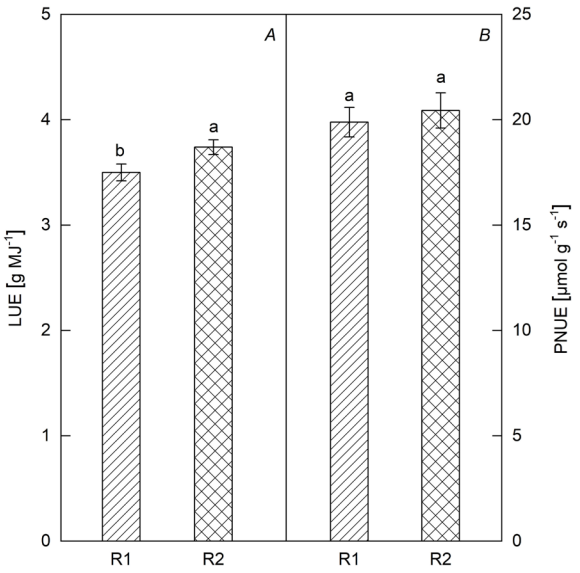

Fig. 6. The light energy-use efficiency (LUE) (*A*) and photosynthetic nitrogen-use efficiency (PNUE) (*B*) of different planting patterns. Data are means ± SE (n = 3), *different lowercase letters* indicate statistically significant differences at the p<0.05 level.

synthetic nitrogen-use efficiency in the leaves of R2 did not increase obviously (Fig. 6*B*).

The absorption, transfer, and conversion of PAR energy are carried out in two photosystems, and the activity of these photosystems affects the efficiency of energy conversion (Matsuoka 1995). The photosynthetic electron transport rate is a comprehensive indicator of the activity of the PSII reaction center, which reflects the photochemical capacity of PAR use (Ji and Jiao 1999). The activities of the photosynthetic carbon assimilation enzymes and photochemical functions of PSII and photosynthetic rate are significantly and positively correlated (Genty *et al.* 1989), and the activities of Rubisco, PPDK, ME, MDH, and PEPC all play important roles in the regulation of photosynthetic carbon assimilation in C_4 plants (Badger and Price 1994, Kromer 1995, Hibberd and Covshoff 2010), which is also regulated by PAR (Stitt and Schulze 1994, Crafts-Brandner and Salvucci 2000, Spreitzer and Salvucci 2002, Chen *et al.* 2014). PAR controls the C_4 PPDK activity in plant leaves, and activity declines under low PAR (Chen *et al.* 2014). In this study, it was found that the activities of these five key photosynthetic carbon assimilation enzymes were higher in R2 plants than in R1 plants between 9:00 h and 16:00 h (Fig. 5), further indicating the contribution of the R2 planting pattern to yield formation. Therefore, the increase in the grain yield in R2 depended on the increased photosynthetic carbon assimilation, which reduced the formation of empty rods and increased the number of stand panicles.

Conclusions: In this study, we designed an optimized wide–narrow planting pattern of maize based on the new idea of the shortest projection length of objects on the ground and the longest illumination periods, which improved PAR for the plant canopy. Based on our results, the photosynthetic performance was enhanced. This observation is reflected by the higher leaf area index, chlorophyll content, photosynthetic rates, and the activities of enzymes related to photosynthesis, which increased ear number and yield. This finding is of great significance for cultivating high-yield maize in northeast China.

References

Alvarez C.E., Detarsio E., Moreno S. *et al.*: Functional characterization of residues involved in redox modulation of maize photosynthetic NADP-malic enzyme activity. – Plant Cell Physiol. **53**: 1144-1153, 2012.

Badger M.R., Price G.D.: The role of carbonic anhydrase in photosynthesis. – Annu. Rev. Plant Phys. **45**: 369-392, 1994.

Bai Y.W., Yang Y.H., Zhu Y.L. *et al.*: [Effect of planting density on light interception within canopy and grain yield of different plant types of maize.] – Acta Agron. Sin. **45**: 1868-1879, 2019. [In Chinese]

Bai Y.W., Zhang H.J., Zhu Y.L. *et al.*: [Responses of canopy radiation and nitrogen distribution, leaf senescence and radiation use efficiency on increased planting density of different variety types of maize.] – Sci. Agr. Sin. **53**: 3059-3070, 2020. [In Chinese]

Chastain C.J., Botschner M., Harrington G.E. *et al.*: Further analysis of maize C_4 pyruvate, orthophosphate dikinase phosphorylation by its bifunctional regulatory protein using selective substitutions of the regulatory Thr-456 and catalytic His-458 residues. – Arch. Biochem. Biophys. **375**: 165-170, 2000.

Chen Y.B., Lu T.C., Wang H.X. *et al.*: Posttranslational modification of maize chloroplast pyruvate orthophosphate dikinase reveals the precise regulatory mechanism of its enzymatic activity. – Plant Physiol. **165**: 534-549, 2014.

Crafts-Brandner S.J., Salvucci M.E.: Rubisco activase constrains the photosynthetic potential of leaves at high temperature and CO_2. – P. Natl. Acad. Sci. USA **97**: 13430-13435, 2000.

Dai M.H., Tao H.B., Wang L.N., Wang P.: [Effects of different nitrogen managements on dry matter accumulation, partition and transportation of spring maize (*Zea mays* L.).] – Acta Agric. Bor.-Sin. **23**: 154-157, 2008. [In Chinese]

Fan X.L., Li F.H., Shi Z.S. *et al.*: [Research on yield increasing effect and physiological characteristics of maize planted in partial ridge-narrow/wide row.] – J. Maize Sci. **18**: 108-111, 2010. [In Chinese]

Gao H.J., Peng C., Zhao Y.M. *et al.*: [Effects of climate, cultivars and density on yield potential of spring corn in northeast of China.] – J. Jilin Agr. Sci. **36**: 4-8, 2011. [In Chinese]

Genty B., Briantais J.M., Baker N.R.: The relationship between the quantum yield of photosynthetic electron transport and quenching of chlorophyll fluorescence. – BBA-Gen. Subjects **990**: 87-92, 1989.

Hammer G.L., Dong Z.S., McLean G. *et al.*: Can changes in canopy and/or root system architecture explain historical maize yield trends in the U.S. Corn Belt? – Crop Sci. **49**: 299-312, 2009.

Hesketh J.D., Musgrave R.B.: Photosynthesis under field conditions. IV. Light studies with individual corn leaves. – Crop Sci. **2**: 311-315, 1962.

Hibberd J.M., Covshoff S.: The regulation of gene expression required for C_4 photosynthesis. – Annu. Rev. Plant Biol. **61**: 181-207, 2010.

Hou J.M., Luo N., Wang S. *et al.*: [Effects of increasing planting density on grain yield, leaf area index and photosynthetic rate of maize in China.] – Sci. Agr. Sin. **54**: 2538-2546, 2021. [In Chinese]

Hu C., Ge J.W., Xu X.N. *et al.*: [Estimation of evapotranspiration and crop coefficient in Dajiuhu peatland of Shennongjia based on FAO56 Penman-Monteith.] – Chin. J. Ecol. **31**: 1699-1706, 2020. [In Chinese]

Ji B.H., Jiao D.M.: [Photochemical efficiency of PSII and characteristics of photosynthetic CO_2 exchange in indica and japonica subspecies of rice and their reciprocal cross F1 hybrids under photoinhibitory conditions.] – Acta Bot. Sin. **41**: 508-514, 1999. [In Chinese]

Jia Y.Y., Xiao W.X., Ye Y.S. *et al.*: Response of photosynthetic performance to drought duration and re-watering in maize. – Agronomy **10**: 533, 2020.

Jin R., Li Z., Yang Y. *et al.*: [Effects of density and row spacing on population light distribution and male and female spike differentiation of summer maize in hilly area of central Sichuan.] – Acta Agron. Sin. **46**: 614-630, 2020. [In Chinese]

Jin S.H., Hong J., Li X.Q., Jiang D.A.: Antisense inhibition of Rubisco activase increases Rubisco content and alters the proportion of Rubisco activase in stroma and thylakoids in chloroplasts of rice leaves. – Ann. Bot.-London **97**: 739-744, 2006.

Kromer S.: Respiration during photosynthesis. – Annu. Rev. Plant Phys. **46**: 45-70, 1995.

Li G., Gao H.Y., Zhao B. *et al.*: [Effects of drought stress on activity of photosystems in leaves of maize at grain filling stage.] – Acta Agron. Sin. **35**: 1916-1922, 2009. [In Chinese]

Li H.S., Sun Q., Zhao S.J. *et al.*: [Principles and techniques of plant physiological and biochemical experiments.] – In: Xue Y. (ed.): [Extraction, Separation and Physicochemical Properties of Chloroplast Pigment.] Pp. 130-135. Higher Education Press, Beijing 2000. [In Chinese]

Li J., Wang H.Z., Liu P. *et al.*: [Differences in photosynthetic performance of leaves at post-flowering stage in different cultivation modes of summer maize.] – Acta Agron. Sin. **47**: 1351-1359, 2021. [In Chinese]

Liang Y., Qi H., Wang J.Y. *et al.*: [Effects of growth and yield of maize under wide and narrow row cultivation.] – J. Maize Sci. **17**: 97-100, 2009. [In Chinese]

Lin T.B., Qu Y.W., Zhang T.X. *et al.*: [Light use efficiency in different canopy layers of *Zea mays* stand.] – Chin. J. Ecol. **27**: 551-556, 2008. [In Chinese]

Liu C.X., Li Z.X., Liu T.S. *et al.*: Impact of genetic background on the leaf-protective enzyme activity and hormone levels of maize. – Agronomy **8**: 234, 2018.

Liu T.D., Song F.B.: [The comparison of photosynthetic characters on ear leaf under different wide–narrow planting patterns in maize.] – Acta Agric. Bor.-Sin. **29**: 117-121, 2014. [In Chinese]

Loomis R.S., Williams W.A.: Maximum crop productivity: An estimate. – Crop Sci. **3**: 67-72, 1963.

Maddonni G.A., Otegui M.E., Cirilo A.G.: Plant stand density, row spacing and hybrid effects on maize canopy architecture and light attenuation. – Field Crop. Res. **71**: 183-193, 2001.

Matsuoka M.: The gene for pyruvate, orthophosphate dikinase in C_4 plants: structure, regulation and evolution. – Plant Cell Physiol. **36**: 937-943, 1995.

Nakamoto H., Edwards G.E.: Influences of oxygen and temperature on the dark inactivation of pyruvate, orthophosphate dikinase and NADP-malate dehydrogenase in maize. – Plant Physiol. **71**: 568-573, 1983.

Reynolds M., Bonnett D., Chapman S.C. *et al.*: Raising yield potential of wheat. I. Overview of a consortium approach and breeding strategies. – J. Exp. Bot. **62**: 439-452, 2011.

Sawada S., Sato M., Kasai A. *et al.*: Analysis of the feed-forward effects of sink activity on the photosynthetic source-sink balance in single-rooted sweet potato leaves. I. Activation of RuBPcase through the development of sinks. – Plant Cell Physiol. **44**: 190-197, 2003.

Shimazaki K.I., Doi M., Assmann S.M., Kinoshita T.: Light regulation of stomatal movement. – Annu. Rev. Plant. Biol. **58**: 219-247, 2007.

Spreitzer R.J., Salvucci M.E.: Rubisco: structure, regulatory interactions, and possibilities for a better enzyme. – Annu. Rev. Plant. Biol. **53**: 449-475, 2002.

Stewart D.W., Costa C., Dwyer L.M. *et al.*: Canopy structure, light interception, and photosynthesis in maize. – Agron. J. **95**: 1465-1474, 2003.

Stitt M., Schulze D.: Does Rubisco control the rate of photosynthesis and plant growth? An exercise in molecular ecophysiology. – Plant Cell Environ. **17**: 465-487, 1994.

Takahashi-Terada A., Kotera M., Ohshima K. *et al.*: Maize phosphoenolpyruvate carboxylase: mutations at the putative binding site for glucose 6-phosphate caused desensitization and abolished responsiveness to regulatory phosphorylation. – J. Biol. Chem. **280**: 11798-11806, 2005.

Tang L., Zhu X.C., Cao M.Y. *et al.*: [Relationships of rice canopy PAR interception and light use efficiency to grain yield.] – Chin. J. Ecol. **23**: 1269-1276, 2012. [In Chinese]

Tsubo M., Walker S., Mukhala E.: Comparisons of radiation use efficiency of mono-/inter-cropping systems with different row orientations. – Field Crop. Res. **71**: 17-29, 2001.

Wang J.Y., Qi H., Liang Y. *et al.*: [Effects of different planting patterns on the photosynthesis capacity dry matter accumulation and yield of spring maize.] – J. Maize Sci. **17**: 113-115, 2009. [In Chinese]

Wei S.S., Wang X.Y., Dong S.T.: [Effects of row spacing on canopy structure and grain-filling characteristics of high-yield summer maize.] – Chin. J. Appl. Ecol. **25**: 441-450, 2014. [In Chinese]

Wu Z.H., Zhang Z.A., Chen Z.Y., Xu K.Z.: [Research on characteristics of canopy structure and photosynthetic characteristic of maize planting in double lines at one width ridge.] – J. Maize Sci. **13**: 62-65, 2005. [In Chinese]

Xiao W.X., Liu J., Shi L. *et al.*: [Effect of nitrogen and density interaction on morphological traits, photosynthetic property and yield of maize hybrid of different plant types.] – Sci. Agr. Sin. **50**: 3690-3701, 2017. [In Chinese]

Xu Z.G., Sun L., Wang H. *et al.*: [Effects of different planting densities on photosynthetic characteristics and yield of different variety types of spring maize on dryland.] – Sci. Agr. Sin. **50**: 2463-2475, 2017. [In Chinese]

Yan Y.H., Yang W.Y., Zhang X.Q. *et al.*: [Effects of different nitrogen levels on photosynthetic characteristics, dry matter accumulation and yield of relay strip intercropping *Glycine max* after blooming.] – Acta Pratacult. Sin. **20**: 233-238, 2011. [In Chinese]

Yang J.S., Gao H.Y., Liu P. *et al.*: [Effects of planting density and row spacing on canopy apparent photosynthesis of high-yield summer corn.] – Acta Agron. Sin. **36**: 1226-1233, 2010. [In Chinese]

Yu Q., Wang T.D., Sun S.F., Ren B.H.: [A mathematical study on crop architecture and canopy photosynthesis II. numerical study.] – Acta Agron. Sin. **24**: 272-279, 1998. [In Chinese]

Zhang C.Y., Bai J., Ding X.P. *et al.*: [Effects of staggered planting with increased density on the photosynthetic characteristics and yield of summer maize.] – Sci. Agr. Sin. **53**: 3928-3941, 2020. [In Chinese]

Zhang Q., Zhang H.S., Song X.Y., Jiang W.: [The effects of planting patterns and densities on photosynthetic characteristics and yield in summer maize.] – Acta Ecol. Sin. **35**: 1235-1241, 2015. [In Chinese]

Zhang R.H., Guo D.W., Zhang X.H. *et al.*: [Effects of drought stress on physiological characteristics and dry matter

production in maize silking stage.] – Acta Agron. Sin. **38**: 1884-1890, 2012. [In Chinese]

Zhao J., Yang X.G.: Average amount and stability of available agro-climate resources in the main maize cropping regions in China during 1981–2010. – J. Meteorol. Res. **32**: 146-156, 2018.

Zheng B., Zhao W., Xu Z. *et al.*: [Effects of tillage methods and nitrogen fertilizer types on photosynthetic performance of summer maize.] – Acta Agron. Sin. **43**: 925-934, 2017. [In Chinese]

Zhu Q.L., Xiang R., Tang L., Long G.Q.: [Effects of intercropping on photosynthetic rate and net photosynthetic nitrogen use efficiency of maize under nitrogen addition.] – Chin. J. Plant Ecol. **42**: 672-680, 2018. [In Chinese]

Zhu Y.G., Dong S.T., Zhang J.W. *et al.*: [Effects of cropping patterns on photosynthesis characteristics of summer maize and its utilization of solar and heat resources.] – Chin. J. Appl. Ecol. **21**: 1417-1424, 2010. [In Chinese]